Hindawi
Mobile Information Systems
Volume 2022, Article ID 8022002, 14 pages
https://doi.org/10.1155/2022/8022002

Research Article

The Spatial Distribution and Evolution of Traditional Villages Based on Remote Sensing Technology

Hongchen Zhang

Design Art College, Xijing University, Xi'an, Shaanxi, China 710000

Correspondence should be addressed to Hongchen Zhang; 20200071@xijing.edu.cn

Received 7 December 2021; Accepted 9 March 2022; Published 12 April 2022

Academic Editor: Muhammad Muzammal

With the rapid progress of the era and the intensification of urbanization, the traditional villages in the fringe areas have become empty villages. Based on the protection of China's long-standing farming culture, the state preserves the traditional Chinese rural characteristics with the support of advocating the development of urbanization in villages; the proposal of the revitalization strategy with Chinese rural characteristics pays great attention to and supports the development of rural characteristics to a great extent. However, China's vast land and resources and the lack of observation technology make most people do not know enough about traditional villages. Based on the rapid development of drones and remote sensing technology in recent years, this article observes the administrative area of A county in the province of A with the support of big data technology. The DEM data taken by drones is the basic data source; that is, within a certain degree of restriction, elevation data (DEM) can realize effective digital simulation. And the current situation of rural settlement space in County A is analyzed through comprehensive technologies such as GIS technology, parametric analysis technology, and landscape pattern index grading; GIS technology can transform data from multiple sources into geographic graphics. And from the perspective of the ecological environment, the geographical, land use, and settlement spatial pattern of the rural settlements in County A are analyzed, revealing that the spatial distribution of rural settlements in County A is affected by the ecological environment. The results of the study show that the classification statistics table of rural residential areas in County A shows that the base number of independent courtyards is particularly large, accounting for about 83% of the total residential areas. The rural residential areas in County A are dominated by single-family clusters and small clusters, which together account for more than 99.1% of the total area. Large- and medium-sized gathering points are relatively small, accounting for only about 0.87% of the number of village gatherings.

1. Introduction

With the acceleration of the times, various factors have made the traditional rural cultural heritage gradually disappear. The state has also given great support to the construction of traditional villages, proposing to carry out urbanization under the preservation of the heritage of the original cultural landscape, and to build a new socialist countryside with Chinese characteristics in an all-round way. However, it was found in the survey that traditional survey protection methods are slow, and the security is not enough, and the collected data is relatively singular and not complete and accurate. This has also caused a serious delay in the implementation of traditional rural construction and protection measures, and there is an urgent need for a comprehensive, efficient, and convenient data analysis and collection method for data investigation and collection of traditional villages. The research in this paper proposes the collection method of cultural landscape data based on UAV remote sensing technology and explores the environmental recognition, extraction, and analysis of a place based on the image data collected by UAV remote sensing. In addition, the results of sample data extraction are compared with on-site exploration results to improve the accuracy of the evaluation results, and finally, the application of the results is analyzed.

The construction of a new countryside is now the focus of building a well-off society in an all-round way under the

support of the state. The country's rural revitalization strategy has greatly improved the development system and provided strong support. However, China has a vast territory. Today, nearly one-half of the population still gathers in the villages of more than 3 million people. As a major agricultural country, China's achievements are obvious to all, but its investigation and collection have always been a difficult task. With the growth of big data technology, UAV remote sensing technology has been able to lead the development with its absolute advantage in image collection, and it has broad application prospects in many fields. Although the remote sensing technology of UAVs has been greatly developed, there are still shortcomings, especially the current state of UAVs in flight is not very stable. Compared with the satellite remote sensing technology platform, the UAV remote sensing technology can obtain more detailed information and data. The intervention of drone remote sensing technology has provided infinite new possibilities for the research of traditional settlement villages.

Many scholars have already discussed the related research content of remote sensing technology and the distribution of traditional villages. Based on the traditional multibeam measurement method, the accuracy is high, but the spatial distribution is uneven. Dong et al. use Beiwan as the research area, use remote sensing data to construct seabed topography, use multibeam data for verification and correction, use distributed computing technology to distribute big data on different computing nodes, and refine and reconstruct the data [1]. As a new type of business, the homestay industry is developing rapidly, driving the regional economy to a new level. Morinda citrifolia is a precious medicinal material with high medicinal value. Studying its suitable ecological conditions can provide a basis for rational development, artificial cultivation, and sustainable utilization. Luo et al. proposed a feasible method to study the suitable regional distribution of Yunnan pine in Sichuan Province. Taking Yunnan pine in Sichuan Province as an example, according to relevant literature, suitable ecological conditions of Yunnan pine, such as altitude, annual average temperature (MAT), annual precipitation, regional slope, slope range, vegetation coverage, and soil type, are analyzed by remote sensing (RS) and GIS. Based on RS and GIS technology, combined with field verification information, extract the suitable distribution area and area of Yunnan pine [2]. Remote sensing provides local, regional, and global observations of seasonal snowfall, providing key information about the process of snow accumulation. Nolin focused on the advancements in instrumentation and analysis technology developed in the past decade. Areas of progress include improved algorithms for mapping snow range, snow albedo, snow grain size, snow water equivalent, melting detection and snow depth, and new uses for instruments such as multiangle spectrometers, scatterometers, and lidars. The limitations and synergy of instruments and technologies are discussed, and the remaining challenges are clarified, such as multisensor mapping, scaling issues, vegetation correction, and data assimilation [3]. Few people pay attention to the housing occupancy rate (HOR). Based on BPA, BF, and HOR, Han et al. proposed a new fine-scale population spatialization method with Beijing six districts as the research area. The results show that the HOR in the center of Beijing is higher than that in the surrounding areas. This study suggests that HOR may be a key indicator for fine-scale population modeling. In addition, the proposed method can be used to generate a fine-scale population grid map and can provide reliable basic data for rapid response and decision-making [4]. Abrishamkar and Ahmadi used the land surface energy balance algorithm (SEBAL) to obtain the actual evapotranspiration (ETa) value in the Nekooabad agricultural and drainage network and the Ben-Saman area in the Gavkhouni Basin of Iran in 2008. To this end, a time series of midresolution imaging spectrometer images from the Terra satellite has been prepared, and the ETa values for each region this year have been estimated. In order to evaluate the performance of the SEBAL algorithm, the algorithm was executed on the Nekooabad agricultural network located in the Najafabad region, with sufficient land information, and three different methods were used to verify the results [5]. The water consumption of a large area of green space is difficult to achieve with traditional methods. Di et al. developed a practical method using remote sensing data from different sources. The green space first comes from the high spatial resolution RapidEye image using the hierarchical classification method. Secondly, an object-oriented classification method is used to identify the main vegetation types of green spaces. Then, the land surface energy balance algorithm is used to invert the regional green evapotranspiration based on the multitemporal Landsat 8 image. Finally, the water consumption patterns of different types of vegetation were analyzed, and the regional water consumption was estimated [6]. Yuan used the basic information of 8353 archaeological sites to describe the region from 9.5 ka BP (ka BP = 0 thousands of years before BP, where "0 BP" is defined as 1950 to 2.3 ka BP extending from the Yanshan Mountains to the Liaohe Plain in northern China (i.e., the Yanliao region). Based on spatial statistical analysis, including the spatial density of the site and the nearest neighbor analysis of the geographic information system, combined with the review of environmental and climate data, this article analyzes the cultural evolution, the temporal and spatial characteristics of archaeological sites, and the background of human activities in the region's climate and environmental changes. The results show that the evolution of prehistoric culture in Yanliao area is extensively affected by climate and environmental changes [7]. The above-described scholars have achieved corresponding results in the research content of related fields. However, it is not easy for most scholars to collect research data, covering a relatively wide area, and it is not easy to obtain complete and effective data. At the same time, it is also easy to cause negligence and omission when a large amount of data appears.

The innovations studied in this article are as follows: (1) Data collection based on UAV remote sensing technology can obtain more detailed image information, easier to distinguish ground objects and has more advantages in the collection of spatial information in traditional rural areas. (2) Based on the ecological perspective analysis of the natural environment, the natural ecological environment has had a

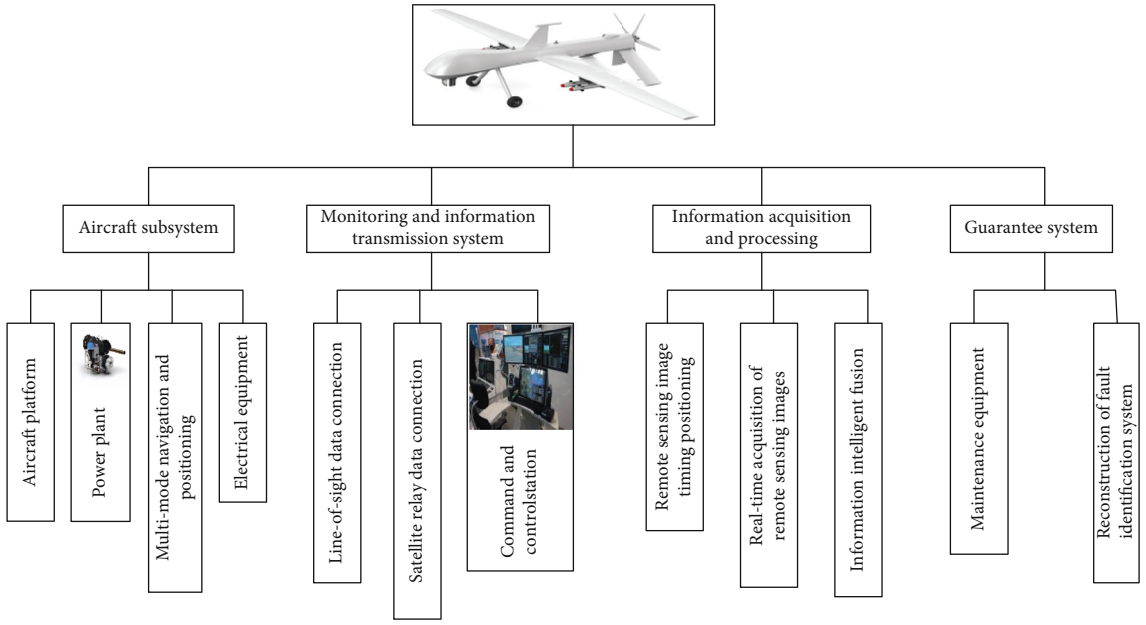

Figure 1: Composition diagram of UAV remote sensing system.

significant and significant impact on the spatial settlement of traditional villages since ancient times.

2. Method on Key Technologies of UAV Remote Sensing System Mapping

2.1. UAV Low-Altitude Remote Sensing System. Combining data transmission, GPS, unmanned driving technology, remote sensing technology (RS), and other related technologies are integrated and used [8] can obtain more intelligent data image resources. In addition, the remote sensing technology is easy and flexible to operate, and the resolution and time phase can be adjusted according to different requirements, making the collection results more diverse and rich [9]. Moreover, the cost of UAV remote sensing technology is lower than that of other remote sensing platforms. It has become one of the current research hotspots of remote sensing aviation technology [10].

A relatively complete UAV remote sensing platform mainly includes four parts, as shown in Figure 1:

Nonmeasurement cameras are often used as aerial photography equipment in UAV remote sensing systems; nonmeasurement cameras refer to cameras that are not designed and manufactured specifically for the purpose of photographic measurement, because the image data collected by nonmeasurement cameras has no film distortion [11]. Poor objective lens distortion is the main factor that affects the errors of the data processing system. The occurrence of this influencing factor will cause the pixel point to shift; that is, the optical distortion will appear [12]. Since the position of the camera shooting equipment in the air is prone to a certain degree of error, which will cause distortion and increase the error of the parameters, as shown in equations (1) to (3), it is necessary to minimize the error on the camera when correcting the camera.

$$\Delta A = (A - A0)\left(R1k^2 + \mathrm{R2k}^4\right) + Q1\left[k^2 + 2(A - A0)^2\right] + 2Q2(A - A0)(B - B0) + \theta(A - A0) + \varphi(B - B0), \tag{1}$$

$$\Delta B = (\mathrm{B} - B0)\left(R1k^2 + R2k^4\right) + Q2\left[k^2 + 2(B + B0)^2\right] + 2Q(A - A0)(B - \mathrm{B0}), \tag{2}$$

$$k = \sqrt{(A - A0)^2 + (B - B0)^2}. \tag{3}$$

2.2. UAV Remote Sensing Data Acquisition Process. The data acquisition process of UAV remote sensing technology is shown in Figure 2.

(1) Generally speaking, the altitude of the drone during flight is related to the focal length of the equipment and the size of the ground resolution, and the altitude of the area is added to the corresponding altitude [13]. Through calculation, the navigation shooting height required by the drone can be obtained:

$$G = \frac{j \times gsd}{b}, \tag{4}$$

$$G0 = G + g. \tag{5}$$

Equation (4) represents j representing the focal length of the shooting device during flight, b representing the phase element size of the equipment mounted, and the calculation result of the ground resolution gsd plus the altitude g of the area; the flying height G of the UAV relative to the ground can be obtained.

(2) For the selected test area, observe the terrain undulations of the area through Google Earth. Google Earth

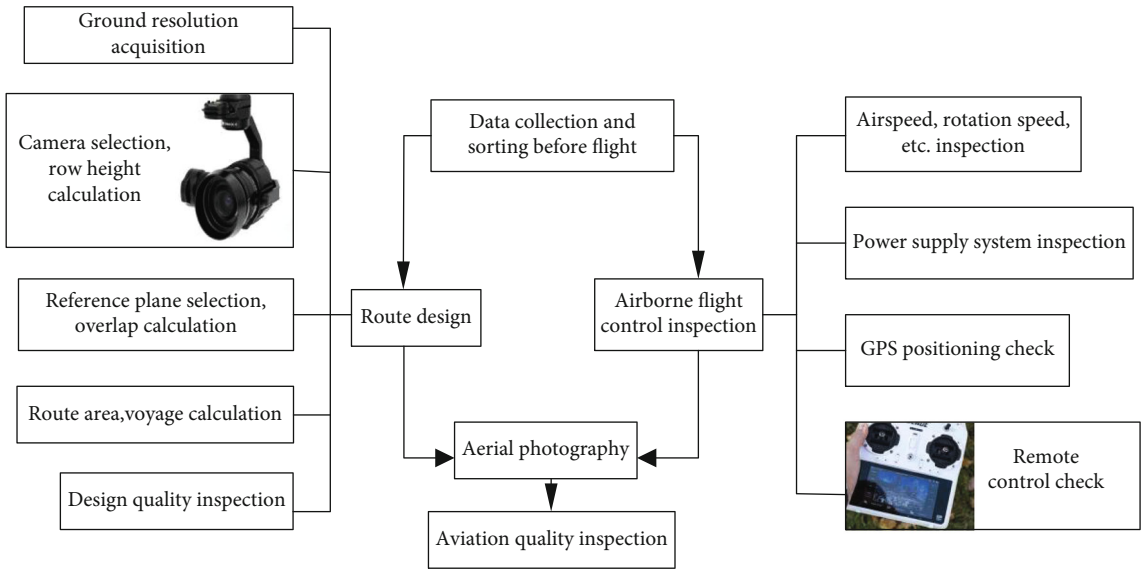

Figure 2: Image acquisition process of UAV remote sensing system.

Observation is a high-definition satellite map positioning software that can observe real images of the earth on a mobile phone and take the average height of the relatively flat place under the area as the base height during the shooting process [14]

Determine on the basis of the benchmark equation:

$$Gji = \frac{\sum_{i=1}^{n} gi}{N}. \tag{6}$$

In equation (6), Gji is the height of the reference plane, and gi is the average height of the flat part of the shooting area.

(3) The degree of overlap of the captured images is determined, and the calculation equation is

$$\begin{aligned} Q^a &= Q^{a'} + \left(1 - Q^{a'}\right)\frac{\Delta g}{G}, \\ P^b &= P^{b'} + \left(1 - P^{b'}\right)\frac{G}{j}. \end{aligned} \tag{7}$$

Among them, P^b, Q^a and $P^{b'}, Q^{a'}$ in the equation, respectively, represent the side and heading overlap degree during the operation of the UAV at the highest point and the datum plane [15].

2.3. The Beam Method Area Network Adjustment of UAV Data Processing. After the distortion is corrected, the air triple encryption can be performed on it [16], which is the main method of processing internal business data, which is also called air triangulation encryption [17]. The quality of the encryption point extraction has a serious impact on the final result, as shown in Figure 3. Air triangulation encryption is a process of matching the same points of multiple images and calculating other encryption points based on the known control point coordinates.

Air triple encryption uses a single image as the reference unit and the collinear equation as the theory of beam method regional adjustment [18]. To settle the external orientation elements of a single image, the equivalent error equations need to be listed according to the internal page encryption and field coordinates.

The calculation model of the adjustment method is shown as follows:

$$\begin{aligned} A &= -j\frac{m1(A - As) + n1(B - Bs) + o1(C - Cs)}{m3(A - As) + n3(B - Bs) + o3(C - Cs)}, \\ B &= -j\frac{m2(A - As) + n2(B - Bs) + o2(C - Cs)}{m3(A - As) + n3(B - Bs) + o3(C - Cs)}. \end{aligned} \tag{8}$$

List the equations that include all control and encryption points, and take the image point coordinates as the observation value, namely:

$$\begin{aligned} UA = {} & m11\Delta As + m12\Delta Bs + m13\Delta Cs + m14\Delta\alpha + m15\Delta\beta \\ & + m16\Delta\chi - m11\Delta A - m12\Delta B - m13\Delta C - lA, \\ UB = {} & m21\Delta As + m22\Delta Bs + m23\Delta Cs + m24\Delta\alpha + m25\Delta\beta \\ & + m26\Delta\chi - m21\Delta A - m22\Delta B - m23\Delta C - lB. \end{aligned} \tag{9}$$

The columns are in matrix form, and the expression equation is

$$\upsilon = [M\ N]\begin{bmatrix} s \\ A \end{bmatrix} - l, \tag{10}$$

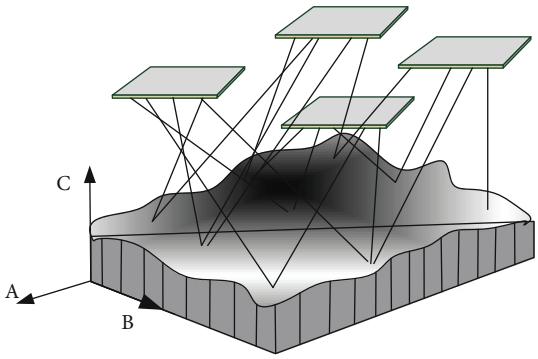

Figure 3: Schematic diagram of aerial triangulation of area network by beam method.

where

$$\begin{aligned} v &= [UA\ UB]^S, \\ M &= \begin{bmatrix} m11\ m12\ m13\ m14\ m15\ m16 \\ m21\ m22\ m23\ m24\ m25\ m26 \end{bmatrix}, \\ N &= \begin{bmatrix} -n11 - n12 - n13 \\ -n21 - n22 - n23 \end{bmatrix}, \\ s &= [\Delta A\ \Delta B\ \Delta C]^S, \\ l &= \lfloor LA\ LB \rfloor. \end{aligned} \tag{11}$$

The combined adjustment equation is

$$\left[M^S M\ M^S N\right][s] = \left[M^S l\right], \tag{12}$$

$$\left[N^S M\ N^S N\right][A] \left[N^S l\right]. \tag{13}$$

The modified equations established by the pixel coordinates are shown in equation (12) and equation (13), and then, the encrypted coordinates are solved, based on the external orientation element.

$$x = \pm \sqrt{\sum_{i=1}^{y} \frac{(\Delta i \Delta i)}{x}}. \tag{14}$$

Finally, the error value can be obtained according to equation (14), which is used to compare the coordinates of the encrypted point and the coordinate of the check point at the same location [19].

3. Research on Rural Gathering Based on Man-Machine Remote Sensing Technology

The test site of this study selected County A under a certain province as the data sampling site.

3.1. The Status Quo of the Social Environment in County A

3.1.1. Location Traffic Overview Based on Man-Machine Remote Sensing Technology. County A covers an area of approximately 2647 km^2, about 76 km from the city's urban area. The county's transportation is convenient. The county's open roads are about 1958.3 km, including 160 km of provincial arterial roads, 245.4 km of county roads, 290.9 km of township roads, and 1262 km of village roads (950 km of cement roads in villages). The highway traffic pattern forms the basic framework, which is mainly manifested in the "four horizontal, four vertical, and eleven external exits" traffic pattern with county roads as the main body, provincial roads as the skeleton, and expressways as arteries [20]. The road construction presents "two transformations," namely, the transformation from quantitative growth to qualitative improvement and the transformation from road network construction to road network improvement [21]. The current status of roads in County A is shown in Figure 4: (a) means national highway, (b) means expressway, (c) means county road, and (d) means village road.

3.1.2. Urban and Rural Development in County A Based on UAV Remote Sensing Technology. According to the 15-year socio-economic development report of County A [22], it is concluded that the total population of County A in 15 years is 2,32095, the permanent population is about 194,467, and the natural population growth rate is 2.08%. The population change from 2010 to 2015 is shown in Figure 5.

As shown in Figure 6(a), the data comparison in the figure shows that the income levels of urban residents and rural residents in County A have increased significantly in the five years from 2010 to 2015 [23]. On the whole, the development of cities and towns is much better than the development of rural areas. However, compared with the average level of City A and Province A, the level income of urban residents in this county is lower, but the income of rural residents is higher than the average level of the province. The specific data comparison is shown in Figure 6(b).

3.1.3. Social Service Infrastructure in County A. County A is making every effort to develop social undertakings. The central kindergarten and middle school in County A have been built and put into use. The smooth integration of educational resources in urban areas has been completed, effectively alleviating the problem of "large class size" in education [24]; that is to say, all classes with more than 46 students in primary and secondary schools belong to the "large class," which also indicates the lack of educational resources and uneven distribution. The provincial education establishment in County A has passed the municipal inspection, and various protection policies that are beneficial to the people's livelihood are being promoted and fully implemented. There are 36 elementary and middle schools in County A (including 1 vocational middle school), and the probability of enrolling school-age children and middle schools at all stages is 100%. There are 13 hospitals and health centers, 267 professional doctors, and 26 individual clinics. The coverage rate of radio and television is 96%.

3.2. Natural Environment Structure Based on UAV Remote Sensing Technology

3.2.1. Geological Structure. The main structural line of County A is from northwest to west, because it is located

Figure 4: The current status of roads in County A: (a) national highway; (b) expressway; (c) county highway; (d) village road.

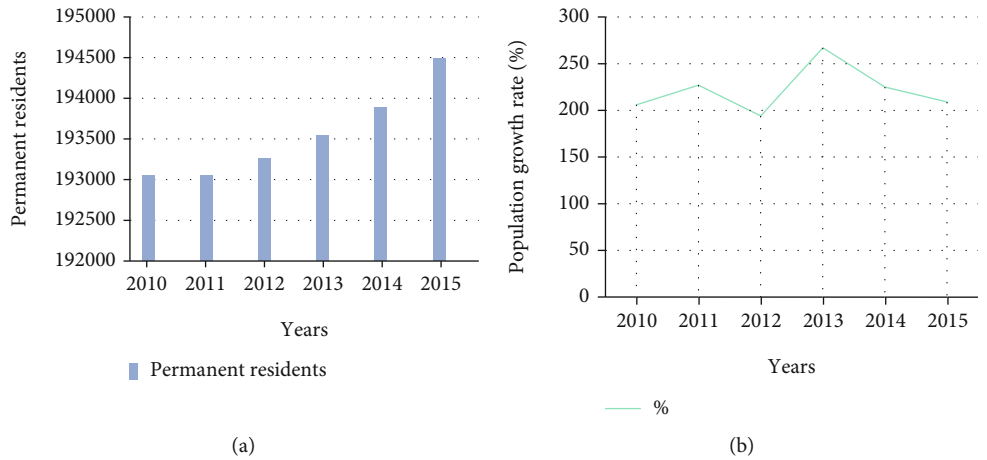

Figure 5: Five-year population change in County A: (a) permanent population; (b) growth rate.

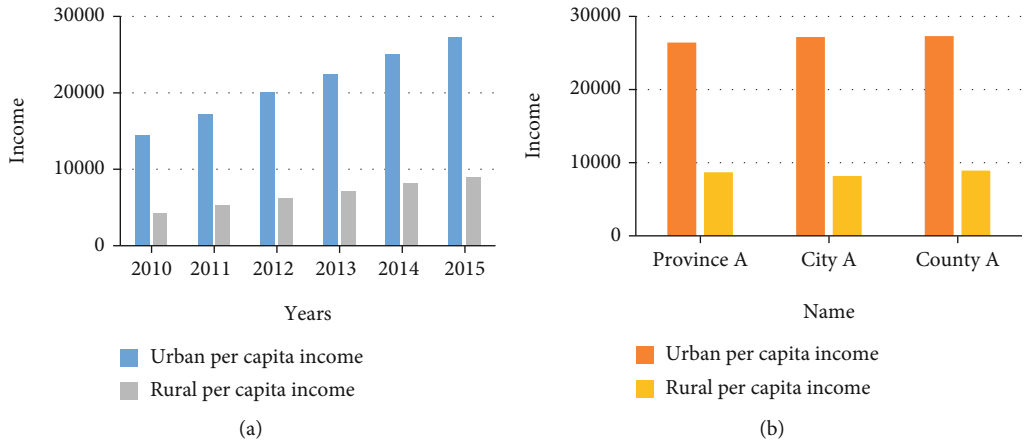

Figure 6: Comparison of residents' income: (a) comparison of incomes in cities and villages in 5 years; (b) comparison of incomes of provinces, cities, and counties.

in the southeast of the Qinling latitude structural system [25]; there are faults from south to north. The occurrence of fault activities is often accompanied by the generation of landslides and debris flows in the region, so the areas with frequent occurrences of faults are often also areas with frequent occurrences of landslides and debris flows [26].

3.2.2. Topography and Landforms in County A. County A is located between 31°37′ and 32°39′ north latitude of the province to which it belongs and is a typical interprovincial border county belonging to the province. On the whole, the landform of County A is in the shape of an irregular inverted triangle, which is narrow in the south and wide in the north. This may be because the county belongs to the Qinling region, which created such a topographic and landform feature [27]. The area of County A is divided into three parts according to the percentage: among them, the mountain occupies the most extensive area, accounting for about 78% of the total area. The second is water, which accounts for about 13.2% of the total area. The last is the area of arable land, which accounts for about 8.8% of the total area.

The altitude within County A is mainly high in the south and low in the north and high in the east and low in the west [28], and the south is dominated by mountains. The terrain classification basis is shown in Table 1.

3.2.3. Zoning of Natural Geological Disasters. Based on the influence of topographical conditions in County A, there are many landslides in the territory, accompanied by a small number of collapses and mudslides. The geological disasters in County A are roughly divided: (1) For high-incidence area, the area is about 23.9% of the county. It covers an area of about 627 km^2 and is mostly distributed in fault fracture zones, river valleys, and middle mountain areas. Human engineering activities are strong. (2) For Zhongfa District, it covers an area of about 55% of the county and has an area of 1445 km^2. The occurrence sites are mostly concentrated in the middle-low and middle-mountainous areas and are distributed outside the northern high-incidence area. (3) For low-incidence area, it covers an area of about 9.7% of the county, with an area of 255 km^2. They are mostly distributed in high-middle and middle-mountainous areas, with relatively few personnel activities. (4) For nonfading area, it is about 11.4% of the county's area. Distributed in high-middle mountainous landforms, mostly natural forests are covered by vegetation.

3.3. Natural Resources Status of County A Based on UAV Remote Sensing Technology

3.3.1. Water Source Basin Resources. The water source basin of County A belongs to the Hanjiang River system in the Yangtze River Basin; among them, the four major rivers of the Han River tributary Ba River, Huangyang River, Lan River, and Ji River all originate in the county, as shown in Figure 7. The basin area accounts for 43.3%, 26.2%, 27.2%, and 3.3% of the county, and the annual surface runoff is 1.391.8 billion cubic meters, which is mostly concentrated in the flood season, accounting for 65%. The county is rich in water resources.

Table 1: Classification basis of topography.

Landform type	Division basis	Area/km^2
Plain basin	Altitude ≤ 600 m	372.6
Low hills	Between 600 and 1000 altitude	939.1
Zhongshan Highland	Altitude > 1000 m	1336.1

3.3.2. Distribution of Land Resources. There are a total of 11 towns under the management of County A. According to the overall land resource utilization plan of County A, the area of agricultural land in the urban area accounts for 9.9% of the county's area, mountain forests account for 84.8%, and grassland accounts for about 0.6%. From the results of these sets of data, the land application types in County A are mainly forest land, supplemented by agricultural land. Based on the current land use status of County A, Table 2 is drawn. The largest farming area is the area where the river flows.

3.4. Rural Aggregation Distribution in County A Based on UAV Remote Sensing Technology

3.4.1. The Current Situation of the Clustering and Distribution of the Villages. There are many rural settlements in the 11 towns under the administration of County A. The total population of the county in 2015 was 232095, among which the rural population was 135,513. The distribution of personnel in each village and town in County A is shown in Table 3.

It can be seen from Table 3 that Town A has the largest rural population in County A, followed by Town K, and Town J has the least.

In summary, the rural settlements mentioned above are mainly concentrated around rivers with sufficient water sources, with the main streams of the Yellow Yang River, Ba River, and Lan River as the main stream. A large number of settlements are also gathered around other tributaries. From the perspective of the number of rural settlements, the rural settlements in County A are mainly distributed in the north, showing a spatial pattern of "density in the north and sparsely in the south." From the perspective of rural population, the distribution of rural population in County A presents a pattern of "more in the east and less in the west."

This research studies the current rural settlements in County A. Because the study area is relatively large, there are many rural settlements, and this study uses rural settlement construction land as the direct research object, the plane layout is adopted as the main classification standard for rural settlements, and the rural settlements in County A are divided into three categories, as shown in Figure 8.

4. Analysis and Results

4.1. Spatial Distribution under the Ecological Environment. The research on the horizontal distribution of rural settlements mainly starts with the spatial distribution of rural settlements in the horizontal direction and analyzes the agglomeration and dispersion of rural settlements in the horizontal direction. The buffer analysis method is used for the river water system to analyze the relationship between

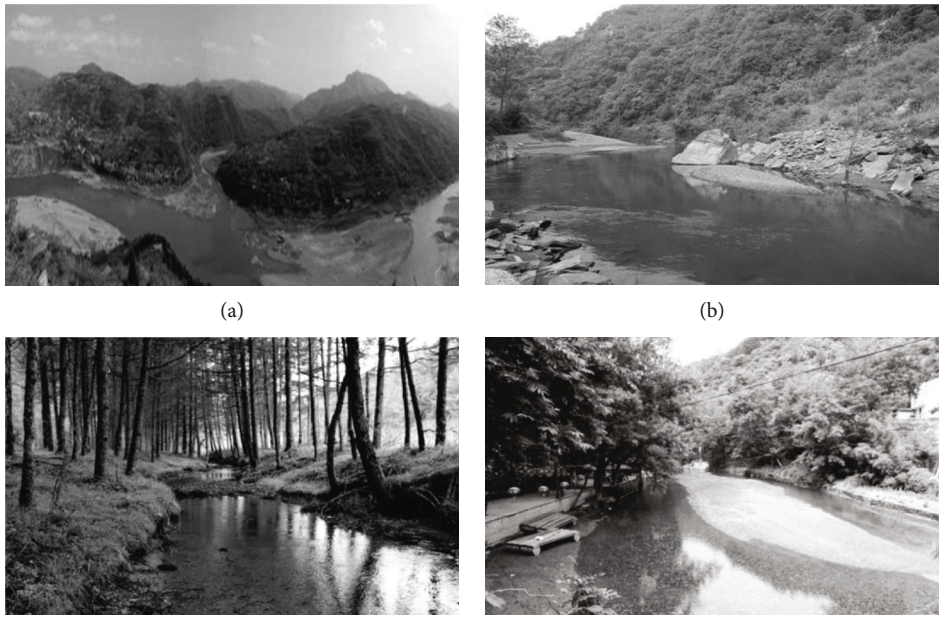

(a) (b) (c) (d)

Figure 7: The source of the four major rivers: (a) Bahe, a tributary of the Yangtze River; (b) Huangyang River; (c) Lanhe; (d) Jihe.

Table 2: Land use status of each town in County A.

Town name	Cultivated area/ km^2	Forest area/ km^2	Grassland area/ km^2
Town A	62.7	190.4	1.26
Town B	18.4	83.2	0.75
Town C	18.2	135.4	1.03
Town D	9.6	170.5	0.85
Town E	14.6	52.4	1.26
Town F	34.6	142.5	1.49
Town G	30.2	297.7	0.85
Town H	56.3	294.3	1.71
Town I	44.3	179.4	2.11
Town J	9.7	380.2	2.53
Town K	24.4	318.3	1.87
Total	322.8	2244.3	15.69

the distribution of rural settlements and the river water system, and the spatial superposition method is used to analyze the topography and landforms and agricultural land.

4.1.1. Horizontal Distribution of Rural Settlements under the Influence of River Systems. ARCGIS 10.2 is used to process the data samples collected under UAV remote sensing technology; it is a geographic information system with strong cloud data processing capabilities and image processing capabilities, combined with the on-site investigation of County A's administrative map and other relevant data, to analyze the water system with multiple ring buffers, and superimpose with settlement patches for statistical analysis. The details are shown in Table 4.

As shown in Table 4, in different buffer zones, the number of village settlements varies greatly. The distribution of rural settlements within 400 meters of the buffer zone accounted for 64.95% of the total. The further away from the river basin, the less the distribution of rural settlements. The overall distribution shows a very obvious downward trend. The distribution of rural settlements is obviously hydrophilic. In the interval 200-400 meters from the river, the number of settlements has decreased the most. From the analysis of the relationship between rural settlements and water systems in County A, the distribution of rural settlements shows a clear trend toward the direction of water sources; that is, the distribution is distorted in the direction of water.

4.1.2. Horizontal Distribution of Rural Settlements under the Influence of Agricultural Land. As shown in Figure 9, the rural settlements in County A are mainly divided into farmland, accounting for 50.04% of the total area of the gathering points, accounting for half of the total area, mainly concentrated and loose settlements. Cultivated land is mainly distributed in relatively flat areas. According to national regulations, the conversion of cultivated land to construction land is strictly restricted, the total amount of construction land is controlled, and special protection is implemented for cultivated land. It is prohibited to occupy cultivated land to build kilns, build graves, or build houses, dig sand, or quarry on cultivated land without authorization. So a large areas of arable land are not classified as residential areas. Therefore, rural residential areas on arable land are mainly distributed in agglomeration areas. There are more and more fallow land in grassland areas, and areas with good geological conditions can be used as construction land, but grasslands are scattered around the cultivated land, and the area is small, so rural settlements are mostly scattered on the grasslands. The woodland area is the largest, mostly in mountainous areas, and the construction conditions are poor, resulting in extremely scattered rural settlements, mostly sporadic settlements. In summary, cultivated

Table 3: Population of each town.

Township	Town A	Town B	Town C	Town D	Town E	Town F
Population	39800	7700	9120	7920	5880	7460
Township	Town G	Town H	Town I	Town J	Town K	
Population	8810	14310	11730	5240	17540	

Category	Feature	Schematic diagram o fsettlement types
Aggregate	That is, farmers gather together around roads, squares, or other public facilities, and use land among each other adjacent, arablel and surrounds the surrounding.It is mainly distributed in areas with relatively flat terrain, arablel and and abundant water sources.The surrounding ecological environment is relatively single, mainly farmland ecological environment	
Loosely agglomerated	The village as a whole is in a reunion shape, separated by roads, rivers or farmland, makingt he existence of households A certain interval. Mainly distributed in river valleys and larger valley areas.The surrounding ecological environment is mostly agricultural mixture of tianand mountain forest ecological environment	
Diaspora	Affected by rivers, roads, and topography, households are scattered in a certain area.Choose multiple farm houses Choose a relatively flat place along ditch, road, etc. The surrounding terrain is more complicated, and the surrounding water sources and arablel and areless. The surrounding ecological environment is mainly mountain and forest ecological environment	

Figure 8: Classification map of rural settlements in County A.

Table 4: Number of settlements in different buffer zones of the river.

River buffer/m	Number of settlements
0-200	7827
200-400	3500
400-600	2165
600-800	1730
800-1000	1373
1000-1200	845

land affects the level distribution of rural gathering points by affecting the development potential and construction conditions of rural settlements.

4.1.3. Horizontal Distribution of Rural Settlements under the Influence of Topography. There are large areas of steep mountains in the southern part of County A, which makes the available farmland and construction land extremely limited, resulting in a low utilization rate. The terrain in the north is relatively flat, with more arable land and abundant water sources, and these water sources are more distributed. Due to the rivers and valleys of the Bashan Mountains in the south, except for a few settlements on the valley terraces, the steep topography of the middle and high mountains severely restricts the gathering and development of settlements. This resulted in extremely scattered distribution of residential areas in the central and high mountains in the horizontal direction. The scale is relatively small, dominated by scattered rural settlements. The northern area of County A has a low elevation and a small slope. Combined with the vertical distribution characteristics of County A, it can be seen that there are more residential areas in low-altitude and low-slope areas. Therefore, the horizontal distribution of settlements in area A is affected by the topography, forming a distribution pattern with more north and less south.

4.2. Spatial Distribution Characteristics of County A Based on UAV Remote Sensing Technology

4.2.1. Vertical Distribution Characteristics of Rural Settlements. Topography is an important factor affecting the distribution of rural settlements, as well as the main factor

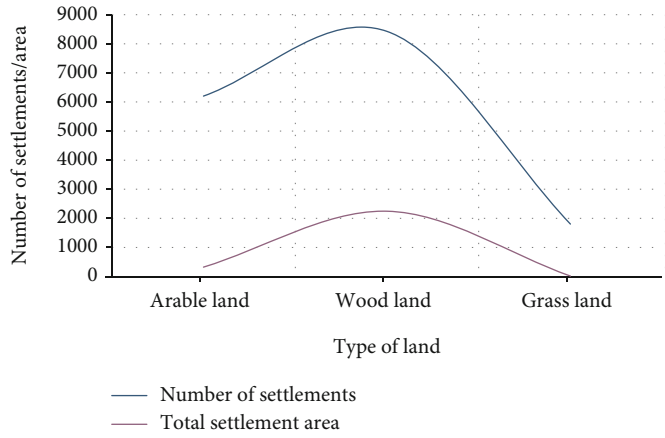

Figure 9: The number and area distribution of settlements of different types of land.

affecting the vertical distribution of rural settlements. The topography and geomorphology factors are subdivided into three aspects: topography, elevation, and slope. Based on the altitude, this study divided the landform types of County A into three categories. The overall topography of County A is high in the south and low in the north, gradually increasing from north to south. Combined with field investigations, plain basins mostly appear in relatively wide river valleys, mostly formed by river impact and siltation. Altitude, slope, and landform type have certain influence on settlement distribution. The statistical analysis results in Table 5.

It can be seen from Table 5 that among the landform types of County A, the area of middle and high mountains is the largest, accounting for 50.83% of the total area of the county, more than half of the total area. However, the number and area of settlement patches on the middle and high mountain landforms are the smallest among the three types of landforms. The smallest area is the plain basin landform. However, the rural settlement area distributed on the plain basin landform is the largest.

It can be seen from Figure 10(a) that the wave crests of the rural settlement patches that vary with elevation are located in the 400-600 m section. This section is a plain basin-like landform with flat terrain and sufficient water sources, which is conducive to settlement development. It can be seen from Figure 10(b) that the peak of the number of settlement patches distributed with the slope is in the range of 15-20°, and the peak of the settlement patch area distribution with the slope is located in the range of 10-15°. Because County A is a mountainous county with horizontal and vertical mountains and rivers, and flat land is rare, rural settlements are mostly distributed in high-slope areas suitable for construction.

4.2.2. Distribution Characteristics of the Spatial Scale of Village Gathering. The total area of rural settlement patches only accounts for 5.61% of the total area of the county. It can be seen that in County A, the rural settlement patches are small in scale and vary greatly in size.

The size of the village clusters is divided into 4 levels, as shown in Table 6.

It can be seen from Table 6 that the statistical table of classification of rural residential areas in County A shows that the base number of clusters of independent courtyards is particularly large, accounting for about 83% of the total residential areas. The rural residential areas in County A are dominated by single-family clusters and small clusters, which together account for more than 99.1% of the total area. Large- and medium-sized gathering points are relatively small, accounting for only about 0.87% of the number of village gatherings.

Combining the distribution of settlements on different landform types, altitudes, and slopes, as shown in Figure 11, rural settlements have the largest scale on flat plains and basins; the lower the altitude and the smaller the slope, the larger the scale of rural settlements. Because County A is a mountainous county with a small area of low-slope land, there is a slight error in the relationship between the settlement land scale and the slope.

4.2.3. Spatial Density Distribution Characteristics of Rural Settlements. Combined with the previous analysis, it can be seen that the spatial density distribution of rural settlements is comprehensively affected by ecological environmental factors such as topography, river systems, and agricultural land. In this study, the spatial density distribution of rural settlements was analyzed using nuclear density estimation method, settlement land proportion analysis method, and cultivated settlement ratio. Kernel density estimation method can be used in probability theory to estimate unknown density function.

According to the previous analysis, the proportion of settlement land uses the ratio of the area of the settlement land to the total area of the study area to express the agglomeration situation of the settlement distribution. The specific expression is

$$\text{Pland} = \frac{\text{Fr}}{r} * 100\%. \tag{15}$$

In the equation, the area of village settlements in County A is Fr, and the total land area is r. According to calculations, the proportion of land used by villages in County A is about 0.56%, and the villages in County A are sparsely distributed as a whole. Dividing County A into three types of landforms, and calculate the proportion of settlement land and the ratio of cultivated accumulation, respectively, as shown in Table 7.

Table 5: The number and area of villages under different topography.

Landform type	Area/ km^2	Number of settlements	Settlement area/ hm^2	Average settlement area/ hm^2	Settlement density/ km^2
Plain basin	372.64	5680	694.3	0.12	15.3
Low hills	939.07	7188	540.2	0.08	7.7
Middle and high mountains	1336.09	3490	246.8	0.07	2.6

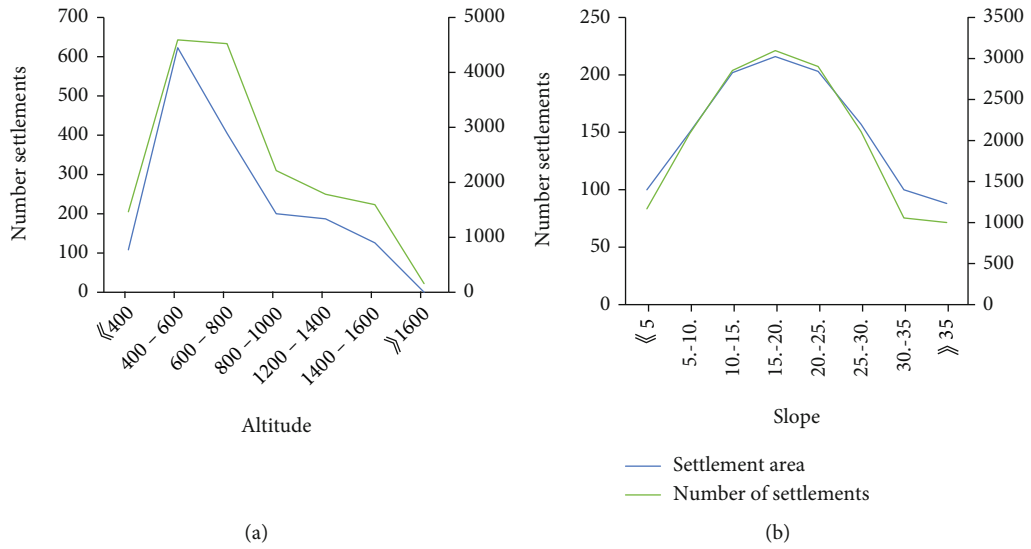

Figure 10: Change trend of the number of settlements: (a) change with altitude; (b) change with slope.

Table 6: Village classification statistics in County A.

Grade	Scope	Number of plaques	The proportion of the number of plaques	Total patch area	Average patch area
Single yard settlement	≤0.1	13634	82.96	237.28	0.04
Small settlement	0.1-1	2660	16.19	612.45	0.23
Medium-sized settlement	1-5	130	0.79	245.75	1.91
Large settlement	>5	13	0.08	89.51	7.46

It can be seen from Table 7 that in the topography of County A, the proportion of residential land in plains and basins is the highest at 1.9%, followed by low mountains and hilly areas at 0.6%, and the middle and high mountain areas are the smallest at 0.2%. The flat basin is relatively sparse, and the low-mountain range is relatively sparse. The middle and high mountain areas have the largest proportion of cultivated land, reaching 59.7, followed by low mountains and hilly areas, while the flat basin has the smallest amount of cultivated land.

4.3. Spatial Distribution Characteristics of Villages from Different Perspectives

4.3.1. The Spatial Distribution Characteristics of Villages under the Ecological Perspective Based on Drone Remote Sensing Technology

(1) Affected by topography and geomorphology, the distribution of rural settlements presents a distribution state of "more in the north, less in the south, low in the more high, less in the north, dense in the north and sparse in the south"

County A is a mountainous county. The mountainous area accounts for more than 80% of the county's total area. The overall terrain trend is "high in the south and low in the north." The distribution of village settlements in County A is normal, with changes in altitude and inclination. Different landform types have different ups and downs, forming different ecological environments and building conditions, thereby affecting the development potential of the gathering point. The flatter the landform type, the more it can withstand higher development needs and the larger the scale of settlements. Therefore, the number of villages with flat plains, basins, and low-mountain hilly landforms is larger, and the scale is larger. Therefore, the rural residential areas present a distribution state of "more in the north and less in the south, and more in the low and high and less in the south."

Affected by the river system, the settlements are distributed close to the river in the form of clusters or loose clusters.

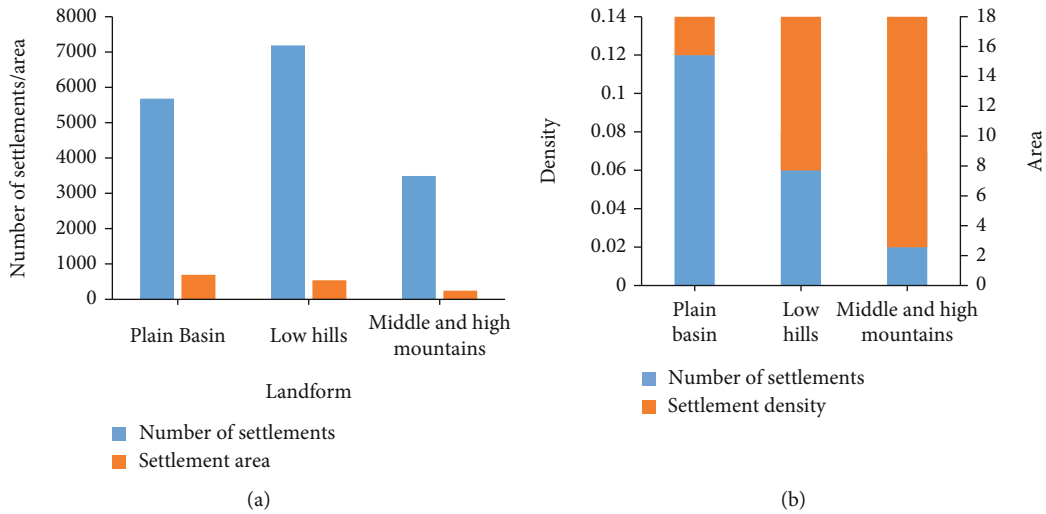

Figure 11: Agglomeration of villages with different landforms: (a) the ratio of the number of settlements to area; (b) the ratio of average area density.

Table 7: Aggregate patches and areas of villages in County A that do not use landforms.

Landform type	Area/hm^2	Settlement area/hm^2	Proportion of settlement land/%	Cultivated area	Tillage ratio
Plain basin	36759	694.3	1.9	9838.8	14.2
Low hills	93407	540.2	0.6	13377.9	24.8
Middle and high mountains	134534	246.8	0.2	14742.8	59.7

Water source is one of the necessary resources for human survival and development, and it is also one of the indispensable conditions for the formation and development of settlements. As the distance from the river increases, the distribution of settlements becomes less and less. However, the water system also poses a certain threat to the safety of residential areas and villagers, and certain protective measures need to be taken, or there is a certain safety distance. With the improvement of technology, this distance can be guaranteed even if it is close to the river. Therefore, the rural settlements that are closer to the river are distributed more, the scale is larger, and the density is higher. Most of the settlements are clustered or loosely distributed along the river.

(2) Affected by agricultural land, rural settlements are mostly distributed on cultivated land in clusters or loose clusters and scattered on grassland and woodland

A large number of settlements are distributed around the cultivated land. As time goes by, the settlements around the cultivated land are mostly settlements or loose settlements. According to the previous analysis, the spatial distribution of rural settlements is not a manifestation of a single form of distribution. The actual distribution of rural settlements is a comprehensive manifestation of various distribution elements. Therefore, under the influence of ecological and environmental factors, the rural residential areas in County A show the spatial distribution characteristics of "more in the north and less in the south, dense in the north and sparse in the south, low in the front and high in the rear" and are densely and loosely distributed around the cultivated land with sufficient water sources.

4.3.2. The Spatial Distribution of Rural Settlements

(1) A large number of rural settlements are still scattered in mountainous areas, with small scale and insufficient concentration. Combining the field investigation and the previous analysis, it can be seen that a large number of rural settlements are still scattered in the mountainous areas. The backward economy and transportation, the complexity of the ecological environment, and the heavy production and labor make it difficult for the settlements in the mountainous areas to gather, most of which are scattered in various valleys and terraces. Due to population exodus, the land is barren, which is not conducive to the development of the village

(2) The coupling between the distribution of village settlements and the ecological environment is not enough. From the perspective of distribution characteristics, a large number of village settlements are still distributed in the mountain forest land in the form of scattered points, and they have not chosen to be distributed in the most suitable environment for development. This has adverse effects on the settlements themselves and the surrounding ecological environment. From the perspective of resource allocation, the distribution of arable land resources and

water resources and residential areas is not in harmony. In the high-altitude river valley area south of the county seat, there is still a large amount of arable land that is idle. In addition, there are many idle houses occupying construction land and even cultivated land, which is a serious waste of land resources

5. Conclusion

The research content of this article first introduces the basic principles and elements of UAV remote sensing technology and conducts a more detailed analysis from the aspects of social infrastructure and natural environmental resources. According to the administrative area map of district A obtained from remote sensing data, the settlement forms of traditional villages are classified, combined with the current population situation and ecological environment, analyze the current distribution of rural settlements in Province A. A better understanding of the location explored in County A will be more helpful for future research. The research results show that the influencing factors of the ecological environment have led to the distribution of "more north, less south, near north, sparse south, and low density/high dilution" in rural residential areas in area A. Most of them are scattered around the cultivated land with sufficient water source, and there is sufficient water source. The aggregation type is mainly manifested in the form of aggregation and loose combination. The base number of single courtyard gathering points is particularly large, accounting for about 83% of the total number of residential areas. Rural settlements in County A are dominated by independent courtyards and small clusters. The current distribution problems are mainly reflected in the following aspects: many rural settlements are still scattered in mountainous areas, and the distribution of rural settlements is not fully matched with the ecological environment. The low mountains in the south are the main rural settlements, and the middle-high mountainous areas are mostly scattered, with rural settlements dominating.

Data Availability

The data used to support the findings of this study are available from the corresponding author upon request.

Conflicts of Interest

The author declares no conflicts of interest.

Acknowledgments

This research study is sponsored by the Scientific Research Fund project of Xijing University. The name of the project is research on landscape gene protection and development of traditional village under the influence of multiple cultures. The project number is XJ210208. The author thanks the project for supporting this article.

References

[1] Y. Dong, B. Q. Hu, S. L. Zhang, Y. L. Huang, G. C. Nong, and H. Xin, "Research on North Gulf distributed big data submarine 3D terrain computing system based on remote sensing and multi-beam," *Soft Computing*, vol. 24, no. 8, pp. 5847–5857, 2020.

[2] Y. Luo, Y.-B. Dong, C. Zhu, W.-F. Peng, Q.-M. Fang, and X. Xin-Liang, "Research on suitable distribution of Paris yunnanensis based on remote sensing and GIS," *China Journal of Chinese Materia Medica*, vol. 42, no. 22, pp. 4378–4386, 2017.

[3] A. W. Nolin, "Recent advances in remote sensing of seasonal snow," *Journal of Glaciology*, vol. 56, no. 200, pp. 1141–1150, 2017.

[4] D. Han, X. Yang, H. Cai et al., "Modelling spatial distribution of fine-scale populations based on residential properties," *International Journal of Remote Sensing*, vol. 40, no. 14, pp. 5287–5300, 2019.

[5] M. Abrishamkar and A. Ahmadi, "Evapotranspiration estimation using remote sensing technology based on SEBAL algorithm," *Iranian Journal of Science and Technology-Transactions of Civil Engineering*, vol. 41, no. 1, pp. 65–76, 2017.

[6] S. Di, Z.-L. Li, R. Tang, X. Pan, H. Liu, and Y. Niu, "Urban green space classification and water consumption analysis with remote-sensing technology: a case study in Beijing, China," *International Journal of Remote Sensing*, vol. 40, no. 5-6, pp. 1909–1929, 2019.

[7] Y. Yuan, "Cultural evolution and spatial-temporal distribution of archaeological sites from 9.5–2.3 ka BP in the Yan-Liao region, China," *Journal of Geographical Sciences*, vol. 29, no. 3, pp. 449–464, 2019.

[8] N. V. Maksyuta, V. I. Vysotskii, S. V. Efimenko, A. S. Sabirov, G. M. Filippov, and I. V. Lysova, "Evolution of the spatial distribution of hydrogen atoms channeling along non-chiral carbon nanotubes," *Techniques*, vol. 13, no. 3, pp. 542–547, 2019.

[9] J. Yang, Q. Sun, H. Yu, K. Ueno, H. Misawa, and Q. Gong, "Spatial evolution of the near-field distribution on planar gold nanoparticles with the excitation wavelength across dipole and quadrupole modes," *Photonics Research*, vol. 5, no. 3, pp. 187–193, 2017.

[10] L. G. Li, P. Y. Zhang, W. X. Liu, J. Li, and L. F. Wang, "Spatial-temporal evolution characteristics and influencing factors of county-scale environmental pollution in Jilin Province, Northeast China," *Ying yong sheng tai xue bao=The journal of applied ecology*, vol. 30, no. 7, pp. 2361–2370, 2019.

[11] E. Sharps, J. Smart, L. R. Mason et al., "Nest trampling and ground nesting birds: quantifying temporal and spatial overlap between cattle activity and breeding redshank," *Ecology& Evolution*, vol. 7, no. 16, pp. 6622–6633, 2017.

[12] Y. Wang, Y. Zhao, and X. U. Xin, "Types, concentration, diffusion and spatial structure evolution of natural gas resource flow in China," *Journal of Resources and Ecology*, vol. 7, no. 1, pp. 12–20, 2016.

[13] J. Li, H. Xu, W. Liu, D. Wang, and S. Zhou, "Spatial pattern evolution and influencing factors of cold storage in China," *Chinese Geographical Science*, vol. 30, no. 3, pp. 505–515, 2020.

[14] E. Doumbia, C. Liousse, S. Keita et al., "Flaring emissions in Africa: distribution, evolution and comparison with current inventories," *Atmospheric Environment*, vol. 199, pp. 423–434, 2019.

[15] N. F. Dotti and A. Spithoven, "Economic drivers and specialization patterns in the spatial distribution of framework programme's participation," *Papers in Regional Science*, vol. 97, no. 4, pp. 863–882, 2018.

[16] Y. Liu, Z. Yang, Y. Huang, and C. Liu, "Spatiotemporal evolution and driving factors of China's flash flood disasters since

1949," *Science China Earth Sciences*, vol. 61, no. 12, pp. 1804–1817, 2018.

[17] Z. C. Chen, X. P. Xie, and M. W. Bai, "Dynamic evolution of wetland landscape spatial pattern in Nansi Lake, China.Ying yong sheng tai xue bao," *Ecology Zhongguo Sheng Tai Xue Xue Hui, Zhongguo Ke Xue Yuan Shenyang Ying Yong Sheng Tai Yan Jiu Suo Zhu Ban*, vol. 27, no. 10, pp. 3316–3324, 2016.

[18] K. M. Pang, N. Karvounis, J. H. Walther, J. Schramm, P. Glarborg, and S. Mayer, "Modelling of temporal and spatial evolution of sulphur oxides and sulphuric acid under large, two-stroke marine engine-like conditions using integrated CFD-chemical kinetics," *Applied Energy*, vol. 193, no. MAY1, pp. 60–73, 2017.

[19] R. N. Andrews, J. Serio, G. Muralidharan, and J. Ilavsky, "An in situ USAXS–SAXS–WAXS study of precipitate size distribution evolution in a model Ni-based alloy," *Journal of Applied Crystallography*, vol. 50, no. 3, pp. 734–740, 2017.

[20] E. M. Korobova, "Principles of spatial organization and evolution of the biosphere and the noosphere," *Geochemistry International*, vol. 55, no. 13, pp. 1205–1282, 2017.

[21] F. J. Lin, Z. H. Chen, X. Q. Li, J. J. Liao, and Y. Zhu, "Generation and evolution of magnetic field in the relativistic plasma following q-nonextensive distribution," *Physics of Plasmas*, vol. 24, no. 2, pp. 022120–022542, 2017.

[22] W. Hui, Q. Xuwen, F. Yuhai et al., "The Application of High Resolution Remote Sensing Technology to Ore-Prospecting in Dahongliutan-Fulugou Area of West Kunlun Mountains," *Geology in China*, vol. 45, no. 6, pp. 1289–1301, 2018.

[23] G. Kim, A. Kim, and Y. Kim, "A new 3D space syntax metric based on 3D isovist capture in urban space using remote sensing technology," *Computers Environment and Urban Systems*, vol. 74, pp. 74–87, 2019.

[24] L. L. Nan, "Retracted article: Agricultural climate change and design of agricultural product e-commerce trading platform based on remote sensing technology," *Journal of Geosciences*, vol. 14, no. 6, pp. 1–14, 2021.

[25] Y. A. Twumasi, E. C. Merem, J. B. Namwamba et al., "Use of GIS and remote sensing technology as a decision support tool in flood disaster management: the case of Southeast Louisiana, USA," *Journal of Geographic Information System*, vol. 12, no. 2, pp. 141–157, 2020.

[26] T. S. Abdulkadir, R. U. M. Muhammad, W. Y. Khamaruzaman, and H. M. Ahmad, "Geospatial assessment of soil moisture distribution in Cameron Highlands using GIS and remote sensing," *Techniques Malaysian Construction Research Journal*, vol. 5, no. 3, pp. 14–27, 2019.

[27] L. Jiao, M. Liang, H. Chen, S. Yang, H. Liu, and X. Cao, "Deep fully convolutional network-based spatial distribution prediction for hyperspectral image classification," *IEEE Transactions on Geoscience and Remote Sensing*, vol. 55, no. 10, pp. 5585–5599, 2017.

[28] Y. Si, H. Wang, K. Cai, L. Chen, Z. Zhou, and S. Li, "Long-term 2006-2015 variations and relations of multiple atmospheric pollutants based on multi-remote sensing data over the North China Plain," *Environmental Pollution*, vol. 255, no. 3, 2019.